Analysis of Spike Electrogenesis of Eel Electroplaques with Phase Plane and Impedance Measurements

NOEL L. MORLOCK, DANIEL A. BENAMY, and HARRY GRUNDFEST

From the Laboratory of Neurophysiology, Department of Neurology, College of Physicians and Surgeons, Columbia University, New York 10032, and the Marine Biological Laboratory, Woods Hole, Massachusetts 02543

ABSTRACT Eel electroplaques provide experimental conditions in which registration of phase plane trajectories (dV/dt vs. V) and impedance measurements with an AC Wheatstone bridge, in conjunction with spike electrogenesis describe quantitatively the ionic processes of the electrogenesis. Thus, these data employing as they do measurements of transients, permit an independent test of the validity of the assumptions which underlie the Hodgkin-Huxley equivalent circuit: independent ionic channels with fixed ionic batteries and exhibiting time-variant conductance changes with different kinetics for the different channels. The analysis accords with earlier findings on voltage-clamped electroplaques and this agreement confirms the validity of the equivalent circuit despite the fact that the current-voltage characteristics of the axons and electroplaques differ profoundly. As for squid axons, the equivalent circuit of the electroplaques has four branches: a capacity and three ionic channels. One of the latter is an invariant leak channel (G_L) of high conductance. A K channel (G_K) is fully open at rest, but rapidly undergoes inactivation when the cell is depolarized by more than 40 mv. G_L and G_K have a common inside negative emf (E_K). A Na channel (G_{Na}) with an inside positive emf (E_{Na}) is closed at rest, but opens transiently upon depolarization.

INTRODUCTION

The findings on voltage-clamped eel electroplaques that were reported from the laboratory earlier (Nakamura et al., 1965; Nakamura and Grundfest, 1965) suggested that further data on the eel preparation might offer an independent test of the postulates of the equivalent circuit of Hodgkin and Huxley (1952), namely, that of independent time-variant ionic conductances with fixed independent emf's. The measurements employed for this purpose and which are described in the present paper were recordings of the imped-

ance changes during the spike of a single cell, measured with an AC Wheatstone bridge (Cole and Curtis, 1939), and of the phase plane trajectories, plotting out the first time derivative of the membrane potential during the spike against the membrane potential (Jenerick, 1963).

These two types of measurements involve only transients. Thus, they are obviously different from those of voltage clamping. Furthermore, the electroplaques exhibit depolarizing K inactivation (Grundfest, 1957; Nakamura et al., 1965) in place of the depolarizing K activation that occurs in squid axons (Hodgkin and Huxley, 1952). Thus, the application of the analysis to eel electroplaques would have the virtue of the ionic components of the spike electrogenesis of these cells having different kinetics from those of the spike electrogenesis of squid axons. Indeed, the occurrence of K inactivation simplified the present analysis.

Another advantage of the preparation is that the electrogenically reactive surface of eel electroplaques is essentially a flat sheet of membrane. The spike electrogenesis, which is due to depolarizing Na activation (Nakamura et al., 1965), can be evoked nearly simultaneously either synaptically, by stimulation of nerve terminals that form a dense population on the reactive surface, or directly, by a current passed outward across this surface (Altamirano et al., 1955). Nearly simultaneous activity of the membrane results in an almost perfect "space-clamped" condition (Hodgkin and Huxley, 1952). This situation facilitated analysis since it permitted use of differential equations which, like the equivalent circuit, are analogous to those employed in voltage clamp studies on squid axons (Hodgkin and Huxley, 1952). Using this equivalent circuit (Fig. 8) and the relation between capacitative and ionic currents (equation 1), the time course and relative magnitudes of the different ionic currents (Fig. 9) and of the conductance changes (Fig. 10) during a spike were calculated. The agreement with the phase plane and impedance measurements is good and thus supports the general validity of the Hodgkin-Huxley analysis of spike electrogenesis.

METHODS

Single electroplaques were isolated by dissection from the caudal portion of the Organ of Sachs (Nakamura et al., 1965). The chamber used was that previously employed for voltage clamp measurements (Nakamura et al., 1965) and is shown diagrammatically in Fig. 1. The isolated electroplaque, which is shaped like a thin rectangular wafer, was sandwiched between two Mylar sheets into which windows 1 mm wide by 3 mm long had been cut. These dimensions are smaller than those of the two major surfaces of the cell and thus the latter formed the barrier between the two sections of the chamber, while both major surfaces were accessible to bathing fluid, to stimulation, and to recording. The caudal, innervated, and electrogenically reactive surface was uppermost, accessible to penetration with microelectrodes.

The two microelectrodes which straddled the reactive membrane were filled with 3 M KCl and were connected through Ag-AgCl wires to a pair of neutralized capacity amplifiers for differential recording against a ground in the bath (Fig. 1, right).

Stimuli were applied to the cell through external Ag-AgCl electrodes which straddled the cell and were coupled to an isolation unit that was capable of delivering up to 20 ma. Despite the large current output, the impedance looking backward into the isolation unit was about 1 MΩ. Thus, the stimulator introduced negligible loading of the system. A second pair of Ag-AgCl electrodes likewise straddled

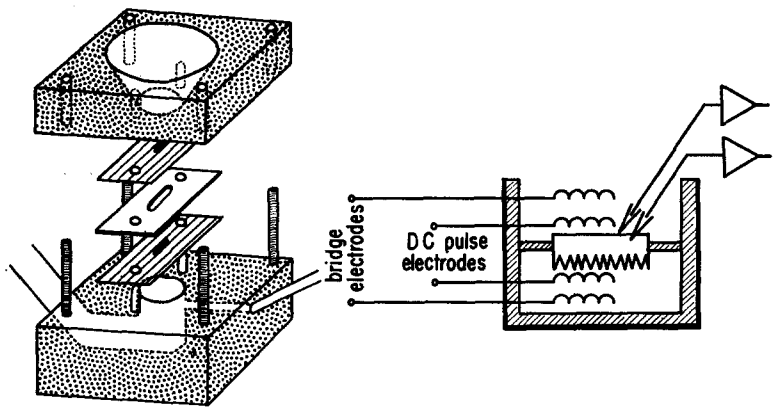

FIGURE 1. The chamber (left) and experimental arrangement (right). The electroplaque formed the partition between two compartments that contained saline. The rostral uninnervated and unreactive membrane, represented by a zig-zag outline was exposed to the lower compartment. The caudal innervated and reactive membrane was uppermost and was straddled by a pair of microelectrodes which led to neutralized capacity amplifiers. Large Ag-AgCl electrodes on either side of the cell were used for applying stimulating currents. A second pair of electrodes led to the AC Wheatstone bridge.

the cell, but were placed more distantly from it than the first pair. They were used to connect the preparation into an AC Wheatstone bridge for impedance measurements. This configuration of the two pairs of electrodes reduced polarization of the bridge electrodes during passage of stimulating currents between the more proximal pair of electrodes.

The impedance bridge is shown schematically in Fig. 2. The fixed arms were 70 kΩ each while the impedance of the cell and electrodes typically was about 200 Ω. Thus, the current through the bridge during the measurements was constant to better than 1:350. The driving voltage caused voltage drops across the innervated membrane that ranged between 0.4 and 4 mv peak-to-peak and these voltages were well tolerated by the cell. The carrier frequency for the bridge ranged between 5 and 20 kHz, but most measurements were made at 10 kHz. The impedance changes observed were independent of the amplitudes of the driving voltages of the carrier frequencies in the ranges used.

The bridge configuration is nonlinear in the range of imbalances that were observed. Furthermore, the change in conductance (G) of the resistive branch of a parallel RC circuit, such as the membrane, and of the real part of the impedance (Z_{real}) are related through a highly nonlinear expression:

$$Z_{real} = G/(G^2 + \omega^2 C^2).$$

The resistance of the membrane of eel electroplaques is very low compared with that of axons (Keynes and Martins-Ferreira, 1953; Altamirano and Coates, 1957. Nakamura et al., 1965). The fluid resistance in series with the membrane and elec-

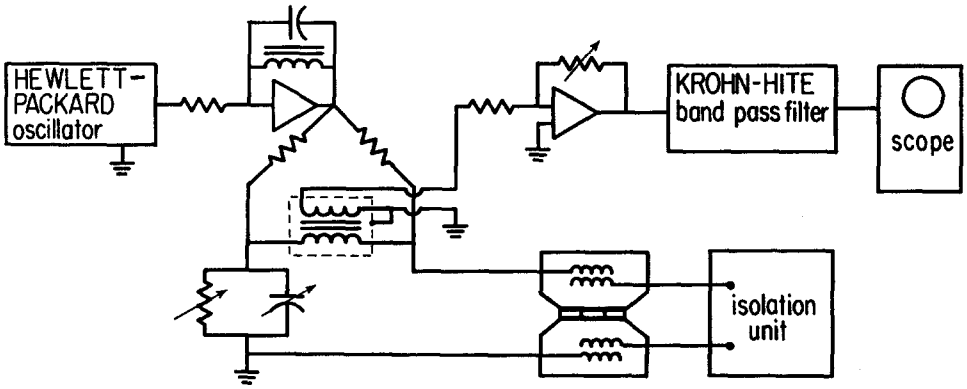

FIGURE 2. Diagram of the impedance bridge and associated equipment. The chamber and electroplaque, shown in the lower right, formed one arm of the bridge. The balancing arm is on the lower left. The oscillator driving the bridge is on the upper left and the recording system is in the upper right.

trodes forms a large and relatively variable part of the total resistance in the bridge arm. Typically, the impedance of the membrane surface exposed in the window was about 3 ω at 10 kHz, while that of the electrodes and fluid was on the order of 100 ω. Under such conditions the absolute values for the resting membrane and for the changes during activity cannot be measured accurately with AC bridge methods (Cole and Cole, 1936), DC measurements with intracellularly applied currents being far more accurate (Tyler et al., 1956). Consequently, the magnitudes of the impedance changes that were observed are relative. Nevertheless, as will be shown below, the impedance data were of considerable importance to the analysis of the spike electrogenesis.

The first time derivative of the spike potential was obtained with the operational amplifier configuration shown in Fig. 3 (Jenerick, 1963). The records in Fig. 3 show Lissajous figures for sine waves of 1 and 20 kHz. These and others made at intermediate frequencies (not shown) exhibited little distortion or tilt, indicating that the operational amplifier configuration employed introduced negligible distortion or phase shift.

Both the impedance and phase plane registration could be made simultaneously

along with the recording of the spike by using a single multiple trace sweep. However, from the point of view of photographic quality it was simpler to make the recordings during successive sweeps, one registering the spike simultaneously with the impedance changes (Fig. 4) and the other recording the spike and the phase plane presentation (Fig. 5).

Spikes were evoked by indirect stimulation (Altamirano et al., 1955) with a brief (0.1 or 0.2 msec) pulse of current flowing inward across the surface of the excitable membrane. Inward current, no matter how strong, does not elicit spike electrogenesis in the electrically excitable membrane component (Altamirano et al., 1955; Nakamura et al., 1965), but it does excite the nerve terminals that lie over the caudal

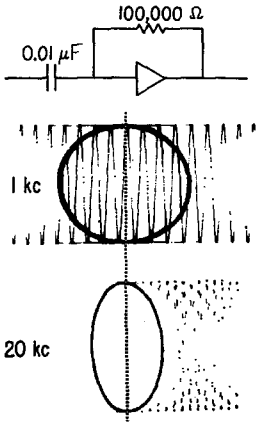

FIGURE 3. The differentiating system for phase plane registration. The operational amplifier (Tektronix Type 3A8, Tektronix, Inc., Beaverton, Ore.) configuration is shown on the top. Below are records of the Lissajous figures obtained with calibrating sine waves at 1 kHz and 20 kHz. A second trace shows the sine waves, but the 20 kHz carrier was poorly photographed because of interference from the chopper frequency of the oscilloscope amplifiers.

surface of the cell and which form a dense population of synaptic contacts with the membrane of the electroplaque. When the pulse is sufficiently strong a large excitatory postsynaptic potential (EPSP) arises nearly synchronously in all parts of the cell after a synaptic delay of about 1 msec (Altamirano et al., 1955). The large, but brief EPSP in turn evokes a spike nearly synchronously over the whole surface. The simultaneous initiation of the spike was essential for the analysis of the measurements, while the synaptic delay between the brief pulse of applied current and the onset of activity allowed sufficient time for large transient artifacts in the measuring system to disappear. The changes in membrane conductance during the EPSP are small relative to those during the subsequent spike, but some distortion of the impedance and of the phase plane registrations was introduced by the EPSP's as will be noted below.

Direct spikes were obtained by reversing the brief current pulses so that the current flowed outward across the excitable membrane of the innervated surface. A strong pulse also evokes the direct spikes nearly simultaneously over the whole surface (Altamirano et al., 1955). However, the stimulus produced a large artifact in the bridge and phase plane recordings that might last as long as 0.5–0.75 msec. Events during the rising phase of the directly evoked spikes thus could not be followed, but direct stimulation was useful in studying events during the falling phase (Fig. 5).

For some measurements, that will be described below, spikes were also elicited with weaker but longer lasting outward currents (Fig. 7). The spike then developed upon a step of depolarization that was maintained as long as the stimulating current was applied (Altamirano and Coates, 1957; Nakamura et al., 1965). In order to measure the resting membrane resistance, small depolarizing and hyperpolarizing pulses were applied.

The preparation was bathed in *Electrophorus* saline (Keynes and Martins-Ferreira, 1953; Nakamura et al., 1965). Complete sets of recordings were made on more than

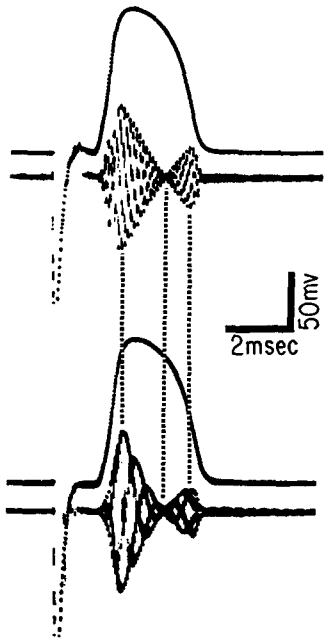

FIGURE 4. Impedance changes recorded simultaneously with an indirectly evoked spike (cell 1, Table I). In the upper record the carrier frequency was 10 kHz. The chopper frequency of the oscilloscope caused the interference pattern of the impedance recording at 20 kHz. Vertical lines connect, respectively, the peaks of the first impedance change (decreased impedance), the troughs where the impedance returned to the resting level, and the peaks of the second impedance change (increased impedance). The intersections of the lines on the lower spike serve to correlate the course of the impedance changes with the time course of the spike.

20 cells and the data on 3 cells were completely analyzed. The results obtained (Figs. 9 and 10, Table I) were so similar in all three cases that it was deemed superfluous to carry through further, time consuming computations. All experiments were done at room temperatures which ranged between 19 and 23°C.

RESULTS

Transient Changes During Spike Electrogenesis

Impedance Changes Typical records of the impedance changes during an indirectly evoked spike are shown in Fig. 4. The carrier frequency was 10 kHz in the upper recording and 20 kHz in the lower. The bridge was initially nulled. The beginning of the change in membrane potential, in this case due to the EPSP, which in turn evoked a spike, was associated with an imbalance of the bridge. The imbalance achieved a peak slightly before the peak of the spike. The bridge output then fell to zero early during the falling phase of the

spike. A secondary imbalance developed which had a peak about halfway on the falling phase, but it subsided very rapidly as the membrane repolarized toward the resting potential.

The vertical lines connect respectively the peak of the first imbalance, the return to zero output, and the peak of the second imbalance in the registrations with the two carrier frequencies. The recording made with the 20 kHz carrier frequency added little to the precision of the measurements. However, the absence of a significant time shift indicates to a close approximation that the bridge imbalances observed represent the real part of the impedance changes.

Measurements that were made with the bridge initially unbalanced showed that the two phases of impedance changes were due to a conductance increase

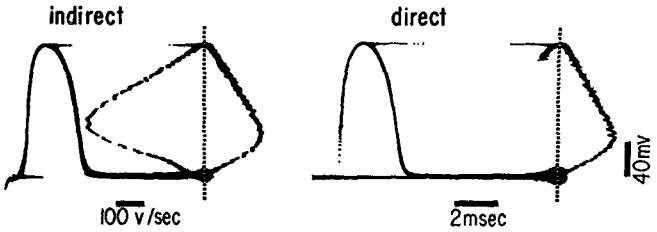

FIGURE 5. Phase plane registrations recorded simultaneously with the indirectly evoked and directly evoked spikes (cell 3, Table I). The abscissa of the phase plane registration is dV/dt. The ordinate is the spike voltage. In the calculations, V is + or − with reference to electrical zero. Further description in text.

and a conductance decrease, respectively. Thus, the initial change corresponds to the phase of increased conductance that was measured by voltage clamping in earlier work (Nakamura et al., 1965) and which was there shown to be due to transient depolarizing Na activation. The second change corresponds to the decrease of conductance in the voltage clamp measurements that results from depolarizing K inactivation.

The impedance data present several new features, since they show the time courses of the changes in conductance during the spike and also, that there is a period during which the conductance returns to the resting value. These changes are presumably correlated with ionic events during the spike, and as will be shown, the impedance data in conjunction with the phase plane data provide sufficient information to specify the nature and time course of the current flow during the spike.

Phase Plane Registrations Simultaneous recordings of the time course of the indirectly evoked spike and the first time derivative of the potential are shown on the left of Fig. 5. The two traces have a common voltage ordinate which is represented by a vertical line that passes through the origin of the

phase plane trajectory. The horizontal excursion in the phase plane registration represents dV/dt. An initial deflection of the trajectory to the left reflects the change in membrane potential during the EPSP. The EPSP itself is seen in the conventional registration as a foot from which the rising phase of the spike develops. The remainder of the phase plane trajectory forms an irregularly diamond-shaped figure, the portion associated with the falling phase of the spike lying to the right of the origin. The vertical line through the origin passes through the curvature that denotes the change in slope at the peak of the spike.

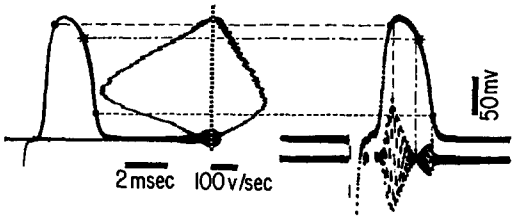

FIGURE 6. Correlation of phase plane and impedance recordings. Same cell as in Fig. 5. The spikes were indirectly evoked. The transition points on the impedance recording are indicated on the spikes and on the phase plane recordings. The potential, V, is given by deflection in the vertical direction; dV/dt by deflection in the horizontal direction.

Similar recordings obtained on this cell following direct stimulation are shown on the right in Fig. 5. As already noted, the large rapid depolarization during the brief applied current introduced a longer-lasting artifact into the phase plane registration so that the recording during most of the rising phase was lost. However, the remainder of the recording duplicates exactly that which was made during the indirectly evoked spike. The identity of the two recordings indicates the absence of propagation, since it would be unlikely that two propagated spikes evoked in different ways would have exactly the same phase relations.

Correlation of Impedance and Phase Plane Data The two sets of data obtained on one indirectly excited cell during two consecutive sweeps are shown in Fig. 6. The phase plane trajectory to the left of the origin coincides with the rise of the conductance to its peak value. The subsequent decline of conductance to the resting value occurs mainly during the curvature of the apex of the phase plane trajectory. These changes are correlated with the onset and decline of Na activation during voltage clamp measurements (Nakamura et al., 1965). However, the secondary impedance increase does not reach its maximum until about halfway during the falling phase of the spike. Depolarizing K inactivation in eel electroplaques begins at about the same membrane poten-

tial as does Na activation, and the K inactivation attains its maximum level within 100 μsec at most (Nakamura et al., 1965; Nakamura and Grundfest, 1965, and unpublished material). Thus, it seems likely that the delay in attaining the peak of the secondary impedance rise is due to persistence of some Na current for more than 1 msec after the peak of the spike.

This conclusion is confirmed by the impedance measurements in Fig. 7, in which a direct spike was evoked by a long-lasting weak outward current for

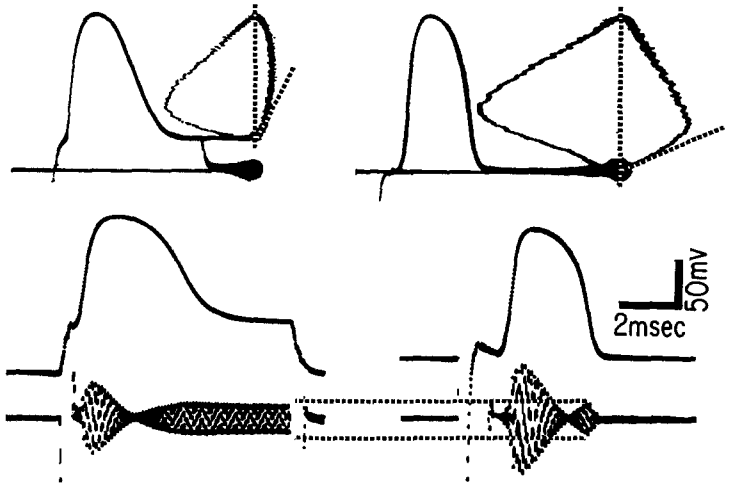

FIGURE 7. Variations of phase plane trajectories (above: cell 3 of Table I) and impedance change (below: cell 1 of Table I) during indirectly evoked spikes (right) and spikes evoked directly by long-lasting outward currents (left). The dotted lines in the phase plane registrations indicate the slopes of the trajectory during the terminal portion of the spike. The dotted line in the lower records indicates that the peaks of the secondary impedance increases in both directly and indirectly evoked spikes are identical. Further description in text.

comparison with the events during an indirectly evoked spike in the same cell. The initial impedance change was smaller and briefer for the directly evoked spike. This was probably due to a combination of two factors. The spike arose out of the voltage step after a delay of about 0.5 msec. Some Na inactivation may have developed during this initial latency. Furthermore, it is also likely that the weak stimulus did not excite the entire membrane uniformly. The deficiency in space clamping is probably also responsible for the slower onset of the peak of the secondary impedance increase. However, once attained the peak value was substantially the same as that during the indirectly evoked spike.

Phase plane trajectories that correspond to the impedance data, but on

another cell are also shown in Fig. 7. In conformity with the smaller initial impedance change during the directly evoked spike, the peak value of dV/dt is considerably smaller than that of the neurally-evoked response of the same cell, although the maximum in both registrations occurs at about the same value of the membrane potential. The changes in the phase plane trajectories during the falling phases of the two spikes are also striking. Their significance will be described below.

Analysis of Spike Electrogenesis

Equivalent Circuit The circuit employed for the analysis (Fig. 8) is formally identical with that of the squid giant axon (Hodgkin and Huxley,

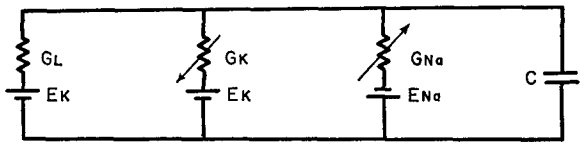

FIGURE 8. Equivalent circuit of eel electroplaque. G_L is the invariant leak resistance. G_K represents the electrically reactive K-permselective channels. G_{Na} represents the Na-permselective channels. G_L and G_K have the same emf (E_K) which is inside negative, while E_{Na} is an inside positive emf. The membrane capacity, like G_L and the emf's is an invariant element.

1952), but the performance of the two electrogenic systems differs in several respects (Nakamura et al., 1965; Nakamura and Grundfest, 1965, and the present work). G_K, the reactive potassium channel, behaves quite differently in the two cells. Whereas in the axon it responds with depolarizing activation, in the electroplaque the response is one of depolarizing inactivation. A rapid, regenerative increase in membrane resistance occurs when the membrane is depolarized by 30–40 mv with a constant current. The G_K channels are also inactivated when the electroplaque is treated with Cs or Rb. This pharmacological inactivation of the G_K channels is evident throughout the whole range of the characteristic, the latter becoming linear for changes in membrane potential of $\pm$150–200 mv, signifying the absence of an electrically excitable component in the steady-state conductance (see Fig. 11 in Nakamura et al., 1965). The unreactive channels are indicated by a constant conductance (G_L) in Fig. 8. The electrically excitable inactivation of G_K is indicated by a downward arrow.[1] The two branches of the steady-state characteristic in the

[1] The terminology of the present paper conforms to that for the squid equivalent circuit (Hodgkin and Huxley, 1952). It differs from the usage of the previous work (Nakamura et al., 1965). The interconversion is as follows, with the earlier usage being indicated by asterisks:

$$G_K^* = G_L; \quad G_L^* = G_L + G_K; \quad G_K = G_L^* - G_K^*.$$

depolarizing quadrant (Nakamura et al., 1965) signify respectively that G_K channels are all open (high conductance state, $G_L + G_K$) or are all closed (low conductance state, G_L).

G_{Na} in the circuit of Fig. 8 is strictly analogous with the same component of the squid equivalent circuit. Na activation occurs when the membrane of the electroplaque is depolarized by 30–40 mv, the range of critical firing level for spike electrogenesis (Nakamura et al., 1965). The depolarizations also induce a slower Na inactivation. G_{Na} is negligibly small in the resting state of the electroplaques and also after Na inactivation is completed; neither of the two branches of the steady-state characteristic is altered when spike electrogenesis is blocked by saxitoxin, tetrodotoxin, or replacement of the Na in the bathing medium with choline or Tris.

As already noted, the voltage clamp measurements showed that depolarizing K inactivation is complete in the electroplaques within about 100 μsec. In the present work, the rapidity of the regenerative change is shown by the subsidence of the secondary impedance increase from its peak within one or two cycles of the 10 kHz carrier frequency, i.e., within 100 to 200 μsec (Figs. 4, 6, and 7). Since the depolarization required for rapidly regenerative K inactivation is about 40 mv, or the same as that required for initiating spike electrogenesis, the G_{Na} and G_K channels are in almost perfect reciprocal relation. During spike electrogenesis the G_{Na} channels are opened, but the G_K channels are closed. As Na inactivation becomes maximal and the G_{Na} channels close, the membrane potential returns toward the resting value. When the depolarization has decreased to about 40 mv the G_K channels again open, likewise regeneratively. During most of the spike the conductance is therefore given by $G_L + G_{Na}$, where G_{Na} is subject to Na inactivation (Nakamura et al., 1965). When a spike is elicited by a long-lasting pulse (Fig. 7, left), the terminal steady-state conductance is only that of the G_L channels, both the G_{Na} and G_K channels being closed by depolarizing inactivation. As demonstrated in the experiment of Fig. 7, the peak increase of impedance during the falling phase of a spike is the same as that during the steady state of a long-lasting threshold applied current.

The equivalent circuit of Fig. 8 differs in another respect from that of the squid axon. In the electroplaques the emf of the G_L channels is the same (E_K) as that of the G_K channels. This identity is evidenced by the findings of the previous work (Nakamura et al., 1965; Nakamura and Grundfest, 1965, and unpublished work). A shift from the high conductance resting state ($G_L + G_K$) to that of low conductance (G_L) did not shift the zero-current origin of the two-branched characteristic, no matter whether the membrane was at the resting potential (-80 to -90 mv) or had been depolarized (to about -10 mv) by elevating the K of the bathing medium.

Ionic Currents When the entire exposed surface of the electroplaque (Fig. 1) becomes active ("space-clamped" condition) the net current is zero. The capacitative current ($I_c = C\,dV/dt$; V is the potential relative to electrical zero at various times during the spike) is then equal and opposite to the sum of the ionic currents (Hodgkin and Huxley, 1952). Since the equivalent circuit of Fig. 8 is formally identical with that for the squid axon, the ionic currents may be expressed by the relations described by Hodgkin and Huxley (1952, p. 505). The sum of the ionic currents is then:

$$C\,dV/dt = -G_L(V + E_K) - G_K(V + E_K) - G_{Na}(V - E_{Na}) \qquad (1)$$

where E_K and E_{Na} are absolute values. When Na activation is instituted there is also rapid K inactivation so that G_K becomes negligible. Then,

$$C\,dV/dt = -G_L(V + E_K) - G_{Na}(V - E_{Na}). \qquad (2)$$

As a result of Na inactivation, G_{Na} becomes negligible during the falling phase of the spike and the conductance falls to its lowest value, G_L, which corresponds to the peak of the secondary impedance increase in Figs. 4, 6, and 7. However, the impedance falls rapidly from this peak signifying that G_K is again coming into play as these channels are opened regeneratively. Then,

$$C\,dV/dt = (G_L + G_K)(-V - E_K). \qquad (3)$$

Thus, during most of the time course of the spike, only one of two voltage-dependent conductances is involved. The phase plane data generate the values of V and dV/dt. G_L and G_K may be obtained in several ways. E_K is the resting potential. As will be described, E_{Na} can be obtained from the combined phase plane and impedance data. Having values for E_K and E_{Na}, equations 2 and 3 can be solved point by point for the voltage-dependent terms G_{Na} and G_K, for the individual ionic currents, and for the changes in total conductance as these parameters vary during most of the spike electrogenesis. Two checks on the validity of the calculations are available: the peaks of the calculated total inward and outward currents should occur at the same time, relative to the spike, as do the negative and positive peaks, respectively, of the phase plane trajectories. The calculated total conductance should show a maximum coincident with the first peak of the impedance measurements and a minimum coincident with the secondary peak of the impedance data.

Computations Examples of the calculations are given in the Appendix. Several starting points are available for the computations. The resting conductance ($G_L + G_K$) can be determined from DC measurements, by applying small brief depolarizing and hyperpolarizing currents. For cell 1 (Table I) such measurements yielded a value of 0.303 mho/cm^2. Larger depolarizing

currents that evoked a spike but outlasted the latter provided the measurements for G_L, which was 0.169 mho/cm² for cell 1. Thus, maximum G_K was 0.134 mho/cm². The time constant ($\tau = RC$) was determined from the phase plane data. As noted above, the terminal portion of the trajectory is linear and represents a constant conductance, $G_L + G_K$ (Fig. 7, right), or only G_L (Fig. 7, left). Equation 3 may be transformed to

$$RC = \frac{V - V_o}{dV/dt} \tag{4}$$

when V_o is either E_K or the steady-state plateau during the applied current (Fig. 7, left). For cell 1 at rest, τ was 190 μsec, whence C was 57.5 $\mu F/cm^2$.

TABLE I

OBSERVED AND CALCULATED PARAMETERS FOR THREE ELECTROPLAQUES AS DETERMINED IN THE PRESENT WORK

Cell no.	Resting potential	Spike peak	G_L	G_K (resting)	G_{Na} (peak)	I_{Na} (peak)	E_{Na}	τ	C
	mv	*mv*	*mho/cm²*	*mho/cm²*	*mho/cm²*	*ma/cm²*	*mv*	*μsec*	*mF/cm²*
1	80	132	0.169	0.134	0.267	29.5	137	190	57.5
2	90	155	0.081	0.101	0.311	25.8	106.5	220	40 (assumed)
3	92	160	0.078	0.129	0.251	22.3	122	193	40 (assumed)
Lowest	72	112	0.08	0.07	0.36	35	26	57	20
Highest	96	152	0.32	0.58	1.25	91	101	150	60

For comparison, the two lower lines give the range of values in Table I of Nakamura et al., 1965. Spike measured from resting potential; E_{Na} from electrical zero.

However, one of the objectives of the present work was to test independently the validity of the steady-state boundary conditions that are assumed in the voltage clamp analysis of spike electrogenesis. In the case of the two other cells for which complete calculations were made, only data from the present transient measurements were used. The time constant was determined in each case from the phase plane trajectory of the indirectly evoked spike, as described above. A value of 40 $\mu F/cm^2$ was assumed for the membrane capacity. As may be seen by inspection of equation 1, the quantity C is a scaling term that determines the absolute values of the conductances, but does not affect their magnitudes relative to each other. Thus, the assumption of the value for C was permissible and, as will be shown, gave reasonably satisfactory results.

The measurement of τ in the indirectly excited cell having produced the value of $G_L + G_K$, G_L was determined from the measurement of τ' in the cell when it was directly excited by a long-lasting current (Fig. 7, left), i.e., when G_L was the only conducting channel. G_K was then obtained by differences.

E_{Na} was also determined from the transient measurements. In the impedance data, it will be recalled (Figs. 4, 6, and 7), the conductance returns temporarily to the resting value early during the falling phase of the spike, when the potential is only somewhat less than that at the peak. Since K inactivation had eliminated the G_K channels, this conductance ($G_L + G_{Na}$) must be equal to $G_L + G_K$, the conductance of the resting cell. Thus, this singular point of the impedance data locates a particular value of the membrane potential at which $G_{Na} = G_K$. Since G_K is already known, E_{Na} can be

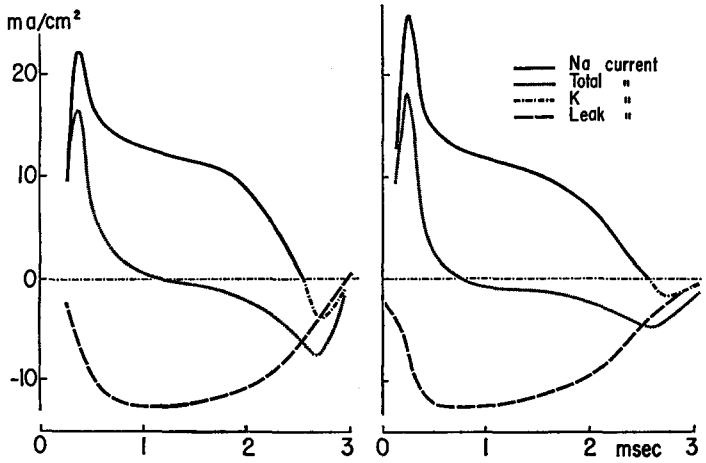

FIGURE 9. Calculated ionic currents during the spike electrogenesis (cell 3 of Table I on left; cell 2 on right).

calculated from the phase plane data for the specific voltage value, by inserting the known value of G_K for G_{Na} in equation 2.

Calculated Currents The ionic currents during the action potentials calculated for two cells are shown in Fig. 9. The individual ionic currents were calculated from equations 2 and 3 and the total current was obtained by algebraic addition. Closely similar data were obtained on the third cell for which computations were made in full. The peak inward and outward total currents coincided within 100 μsec, with the positive and negative peaks registered in the phase plane trajectories. The large leakage current of the eel electroplaques was also found by voltage clamp data (Nakamura et al., 1965). There is only a very small and late component of outward K current during the spike. As already noted above, when the Na current is terminated by full Na inactivation the G_L channel alone carries current, but the regenerative increase in G_K soon permits additional current flow through the K channels.

It is obvious that there are exponential time courses in the falling phase of the total inward current and in the rise of the total outward current. This is

also the prediction of the linear phase plane trajectories (Figs. 5–7), as was noted by Jenerick (1963). However, it must be emphasized that linearity of the trajectory does not imply a constant total conductance except in the case where the system has a single emf. Even with the simplified conditions that prevail in eel electroplaques there is a constant total conductance only during the linear terminal portion of the phase plane trajectory (Fig. 7), since only G_L and G_K are involved and both have the same emf (Fig. 8).

Calculated Conductance Changes In Fig. 10 are shown the impedance registrations for two cells during indirectly evoked spikes. The dotted lines show the conductance changes that were calculated for the same cells. The envelopes of the calculated and observed changes do not coincide because, as

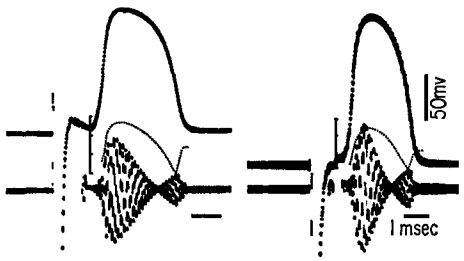

FIGURE 10. Comparison of observed impedance changes and calculated conductance changes during the indirectly evoked spikes of two electroplaques. The records on the left are for cell 1 of Table I; those on the right are for cell 3 of the Table. The time scales (1 msec in both) are somewhat different, but the amplitude scales are the same. The dotted lines show the calculated values. Further discussion in text.

noted above, the impedance recordings are nonlinear. Hence, only the phase relations of the two curves are significant. The resting conductance (G_L + G_K) is shown by the flat portion at the end of each computed curve. This value is actually attained during the terminal portion of the spike, which in the phase plane trajectory is the branch of constant total conductance (Fig. 7, right). The change from the calculated minimum of conductance (which coincides with the peak of the secondary impedance increase) to the high conductance resting state occurs within less than 200 μsec. There is good temporal approximation of the peaks of the calculated conductance increase and decrease with the recorded peaks of the initial impedance decrease and late impedance increase for both cells, although the spikes of the two cells are markedly different (Fig. 10).

The initial portion of the impedance registrations in Fig. 10 includes a conductance increase that is due to the EPSP, which must rise to a depolarization of about 40 mv in order to trigger the neurally evoked spikes. The calculations of the conductances from the phase plane data, however, are based only on the electrically excitable components that alone are present in the equiva-

lent circuit of Fig. 8. Thus they do not encompass the electrically inexcitable synaptic electrogenesis. For this reason the calculations of Figs. 9 and 10 were restricted to that portion of the rising phase of the spike that exceeded 40 mv. Even with this restriction, however, the initial portion of the calculated conductance was lower than the calculated resting conductance for all three cells that had been fully analyzed in the present work.

The discrepancy may be regarded as a systematic error in the analysis. There is, however, a strong possibility that the calculated value is significant. The potential that the EPSP must attain in order to trigger a spike is also that at which regenerative K inactivation is very rapid. Thus, the depolarization caused by the EPSP increases the membrane resistance by eliminating G_K. The load on the synaptic generator is thereby decreased and the depolarization that is due to the synaptic electrogenesis is thereby increased further. This interaction increases the effectiveness of the EPSP in initiating the more slowly developing electrically excitable Na activation and the increase in G_{Na}. Prior to the rise in G_{Na}, however, the conductance of the membrane must have been diminished by K inactivation.

Thus, the early conductance changes probably reflect a net change that includes an increase in conductance due to the EPSP and a decrease due to depolarizing K inactivation. The calculated conductance at a depolarization of about 40 mv on the rising phase of the spike is about halfway between the lowest value (G_L) and the resting value ($G_L + G_K$). This suggests that the conductance component due to the EPSP is of the order of 0.06 mho/cm^2, half the average G_K in Table I. However, direct measurements of the conductance changes during the EPSP are as yet unavailable.

DISCUSSION

The phase plane trajectories during spike electrogenesis constitute the major data in the present work. The impedance data, however, contribute several important items of information. The demonstration (Fig. 7) that the peak of the conductance decrease is the same during the spike as during the plateau of a long lasting depolarizing current that is just threshold for the spike establishes the duration of the Na activation phase and confirms earlier findings regarding the change in conductance that is caused by depolarizing K inactivation. The singular point during the spike, at which the conductance equals the resting value, provides a means for calculating E_{Na}.

Data obtained from measurements of transients naturally emphasize time relations. The peaks of the calculated inward and outward currents fit (Fig. 9) the observed positive and negative maxima of the phase plane trajectories (Figs. 5–7) within a tolerance of about 100 μsec. The calculated conductance changes during the spike also fit very closely the maxima and minima of the impedance changes observed in the Wheatstone bridge meas-

urements (Fig. 10). The calculations were based on the postulates of the equivalent circuit designed for the squid axon (Hodgkin and Huxley, 1952), but adapted to the special properties of eel electroplaques as revealed by the earlier voltage and current clamp data (Nakamura et al., 1965). However, the measurements of the present work are quite different in nature from those of the earlier work. The electrogenic system of eel electroplaques is also different from that of squid giant axons. Thus, the good fit between calculations and measurements observed in the present work provides an independent confirmation of the general validity of the assumptions on which Hodgkin and Huxley (1952) based their equivalent circuit.

The confirmation is all the more impressive since the impedance changes during the spike of eel electroplaques differ so markedly from those that occur during the spike of the squid axon (Cole and Curtis, 1939). In the latter, the conductance rises to a peak at about the same time, or even slightly after the peak of the spike (Hodgkin and Huxley, 1952, Fig. 16). Thereafter it falls monotonically to the resting value, remaining high during the early part of the after-hyperpolarization, until a very late secondary decrease in conductance (initial after-impedance, Shanes et al., 1953). In the electroplaques the conductance attains its maximum value prior to the peak of the spike (Fig. 4) and declines back to the resting value early during the falling phase, while the spike is still only some 15–20 mv below its peak. The conductance continues to fall below the resting value while the membrane is still depolarized by about 60 mv, but it returns rapidly to the resting level before the spike is terminated and remains at this value. As already noted, these changes are predictable, not only from the equivalent circuit and the present measurements, but are also in accord with the voltage clamp data (Nakamura et al., 1965; Nakamura and Grundfest, 1965, and unpublished data).

There is a general similarity between the calculated total ionic current of the electroplaque (Fig. 9) and that during the spike of the squid axon (Hodgkin and Huxley, 1952, Fig. 18). This similarity leads to spikes of rather similar form. The components of the ionic current are, however, markedly different. In the squid axon, the main outward current flows through the electrically excitable K channels. In the eel electroplaque the efflux is predominantly through the passive G_L channels, which have a very high conductance as compared with the low conductance of the leak channels in the axon.

The major differences between the electrogenic processes of squid axons and eel electroplaques stem from the difference in the behavior of the G_K channels. Most, if not all, the current-voltage characteristic of the axon in the region of the zero-current origin is generated by G_L channels, as is revealed by the conditions under which hyperpolarizing responses are elicited in these as well as in other axons (Grundfest, 1961, 1966 *a*, 1967). In eel electroplaques, however, the resting state characteristic is generated by the $G_L + G_K$ channels,

both of which have a high conductance. The axons exhibit depolarizing K activation, their G_K channels opening progressively as the membrane potential is altered in the depolarizing direction. The electrogenic effects of the K activation are degenerative. The K inactivation of the electroplaques, on the other hand, gives rise to a negative slope region of the characteristic. The K inactivation process thus is regenerative and all-or-none. As a consequence, there is no current flow in the G_K channels once the cell is depolarized by more than about 40 mv, the outward ionic current being carried through the G_L channels. Only after the spike has subsided to a depolarization below about 40 mv do the G_K channels come into play again. Reopening of these channels develops along the negative slope characteristic, but in the reverse direction, and K activation thus is likewise regenerative. The rapidity of this regenerative change is shown by the rapidity with which the impedance declines from its peak value to the resting level (Figs. 4, 5, 7, and 10) and is reflected by the time elapsed (<100 μsec) between the termination of the calculated Na current and the peak outward total current (Fig. 9).

The traverse of the negative slope region in the reverse direction is also reflected in the finding that the total outward current *rises* as the spike voltage falls toward the resting potential. This finding is also consistent with the equivalent circuit (Fig. 8). At the secondary impedance peak both the Na and K channels are closed. The charge on the membrane capacity is then dissipated across G_L . However, as the potential falls K channels are opened. The total conductance is now $G_L + G_K$, where G_K is rapidly increasing toward its resting value. This behavior is not seen in the total ionic current of squid axons (Hodgkin and Huxley, 1952, Fig. 18).

The reciprocity between Na activation and K inactivation does not signify that the two cations are carried by the same membrane sites which at different times perform as permselective channels for different ions because of different macromolecular configurations. The process of depolarizing K inactivation is independent of Na activation or Na inactivation. The blocking of Na activation, by pharmacological agents, by depolarization with currents, or by addition of K to the medium does not alter the relations between G_L and G_K, nor does blocking of the G_K channels by Cs or Rb affect the G_{Na} channels (Nakamura et al., 1965; Nakamura and Grundfest, 1965, and unpublished material). If Na and K were transported through the same channels some interaction, reflected in over-all conditions, might be expected. It seems likely that the closeness of the thresholds for Na activation and K inactivation gives rise to the apparent reciprocal linkage.

The replacement of K activation of the axon with K inactivation in eel electroplaques appears to have adaptive significance. The absence of K activation eliminates a degenerative electrogenic component and maximizes the voltage output of the electric organ (Nakamura et al., 1965). However, as

already noted above, the depolarizing K inactivation appears to have another adaptive feature. As the depolarization produced by the EPSP approaches the critical firing level for the spike, K inactivation is rapidly instituted. The heavy loading of the synaptic generator by the very low membrane resistance of the resting cell is then decreased to approximately half. The K inactivation thus causes an amplification of the effectiveness of the EPSP as the initiator of spike electrogenesis. Thereby it accelerates the onset of a spike over the whole electrogenic surface, the desideratum for an efficient electric organ (Grundfest, 1957; Bennett and Grundfest, 1961; Bennett, 1961).

All the reactive K channels are also closed by depolarizing K inactivation in the electroplaques of some of the weakly electric gymnotid fishes, with the transition between maximum and minimum steady-state conductances being through a negative slope region of the voltage-current characteristic (Bennett and Grundfest, 1966). This also appears to be the case in frog muscle fibers that are maintained in isosmotic K_2SO_4 (Adrian, 1964). As in eel electroplaques (Nakamura et al., 1965), pharmacological K inactivation by Rb abolishes a negative slope characteristic in the muscle fibers. The steady-state conductance assumes a single low value identical with that during depolarizing K inactivation. The effect of pharmacological K inactivation is all the more impressive in the frog muscle fibers because the fibers, whether bathed in K_2SO_4 or in the normal saline, exhibit a marked conductance increase in response to hyperpolarizing stimuli (hyperpolarizing K activation; Grundfest, 1961, 1966 *a*). This response is greatly reduced or abolished by substituting the Rb for K (cf. Grundfest, 1966 *b*, Figs. 13 and 14).

Depolarizing K inactivation probably has the same adaptive values in the electroplaques of the weakly electric fishes as it has in the eel. It seems unlikely, however, that K inactivation can play the same role in the muscle fibers. It is likely, rather, that its occurrence in the muscle fiber as well as in puffer neurons (Nakajima and Kusano, 1966) and squid axons (Ehrenstein and Gilbert, 1966) reflects a general feature of the responsiveness of electrically excitable membranes (Grundfest, 1961, 1966 *a*). The difference is that in the electroplaques K inactivation is functionally useful. Thus, it is a prominent response that can be demonstrated during spike electrogenesis (Bennett, 1961; Bennett and Grundfest, 1959, 1966; Nakamura and Grundfest, 1965; Nakamura et al., 1965, and the present work).

Phase plane trajectories in a number of cells were rather less regular than those illustrated in Figs. 5–7. The causes of the irregularities were not investigated. However, it seems likely that a major element was nonuniformity in the phase relations of the spikes at different regions of the membrane. Although spikes that are initiated by strong neural or direct stimuli develop nearly simultaneously over the whole excitable membrane of the cell and thus have nearly the same form at different recording loci (Altamirano et al.,

1955), irregularities are introduced when the tips of the recording microelectrodes that straddle the reactive membrane are somewhat separated (Altamirano et al., 1955, Fig. 17 *A″–C″*). These irregularities are due to the specific properties of the electroplaques, namely their high membrane conductance, small space constant and very large current flow during spike electrogenesis. Although the irregularities may not be readily visible in the recording of the spike, they are accentuated in the phase plane trajectories.

As already noted, absolute measurements of the resting impedance, or of the steady-state impedance during K inactivation by AC applied with external electrodes, are subject to considerable error. Fortunately, the computations of the present work do not depend upon the absolute values, except through the membrane capacity, which is a scaling term. As shown in Figs. 9 and 10, the phase relations of the computed inward and outward currents and of the computed conductances were in good agreement with measurements even when a value for the membrane capacity was assumed, rather than measured directly.

Except for two of the membrane parameters, the values calculated from the transient analyses of the present work (Table I) fall within the range of values that had been obtained in earlier work (Nakamura et al., 1965). The values of E_{Na} calculated for the three cells in the present work were higher than the highest values of E_{Na} as determined earlier. However, the spikes, as measured in the present work, had large amplitudes and it is unlikely that smaller values of E_{Na} could yield the large overshoots that were observed. The time constant was also consistently larger in the present work and showed relatively little variation, whereas it ranged between 57 and 200 μsec in the earlier data (Nakamura et al., 1965). However, the determination of time constants with square pulses is subject to considerable error, and it is perhaps significant that the membrane capacity as calculated in the earlier work also varied widely.

It has been shown that G_L must carry large outward currents during the spike (Fig. 9). It is likely therefore that K is the major carrier of this current. Both G_L and G_K thus must be regarded as K channels, at least formally. However, it must be also assumed then that the macromolecular configuration of the reactive K channels differs from that of the unreactive ones. The "leak" K channels do not discriminate among K, Rb, and Cs since neither G_L nor E_K are affected by substitution of one ion for another, whereas both Cs and Rb act on G_K and induce the same degree of K inactivation as does depolarization by an applied current (Nakamura et al., 1965; Nakamura and Grundfest, 1965, and unpublished data).

The very large values of G_L in the electroplaque in comparison with the low values in most other excitable cells are noteworthy. In a membrane of high resistance it is possible that the leak conductance might be due to permeation of ions through the bulk, lamellar phase of the membrane, through which most

of the water movement probably occurs (Grundfest, 1963, 1966 *a*, 1966 *b*). It seems unlikely, however, that permeation of K ions across the bulk phase could differ widely in different cells. It is rather more likely that in the electroplaques, at least, both G_L and G_K are each constituted by specialized channels, one (G_L) being unreactive to stimuli and, as noted above, rather nonselective for the monovalent cations K, Rb, and Cs. The reactive channels (G_K), are normally open, are specifically K-permselective and are closed by depolarizing stimuli and by Rb or Cs.

At first glance it might be supposed that the high leak conductance is associated with the high membrane capacity of the electroplaques. This does not necessarily follow (Grundfest, 1966 *a*). In many muscle fibers (Katz, 1966) and in some neurons, the membrane capacity is very high, and in sympathetic neurons of frog (Nishi et al., 1965) it may be of the same order as in the electroplaques. In muscle fibers the resting conductances are considerably lower, by as much as three orders of magnitude, although the membrane capacity is high.

APPENDIX

EXAMPLE OF CALCULATIONS; CELL No. 3

Definitions

1. V, potential ($\pm$, referred to electrical zero) measured at any time t during spike.
2. E, fixed emf (absolute values) of an ionic battery (K or Na).
3. I, negative for inward current.
4. dV/dt, positive for rising phase (left of V ordinate in Fig. 5).

Steady-State Values

1. $E_K = 92 \times 10^{-3}$ v (measured resting potential).
2. $C = 40 \times 10^{-6}$ F/cm² (assumed value).
3. τ, resting $= RC = \dfrac{C}{G_L + G_K} = 193$ μsec;

$$-\tau = \frac{-83 \text{ v/sec}}{(-76 + 92)\cdot 10^{-3} \text{ v}} = -193 \text{ μsec (Fig. 7 right and equation 4).}$$

4. $G_L + G_K = \dfrac{C}{\tau} = 0.207$ mho/cm².
5. τ', for cell depolarized by 44 mv $= R'C = \dfrac{C}{G_L} = 514$ μsec;

$$-\tau' = \frac{-31 \text{ v/sec}}{(-27.4 + 44).10^{-3} \text{ v}} = -514 \text{ μsec (Fig. 7 left and equation 4).}$$

6. $G_L = \dfrac{C}{\tau'} = 0.078$ mho/cm².

7. $G_K = 0.129$ mho/cm².
8. Calculation of E_{Na}; $G_{Na} = G_K$ at $V = 49.2 \times 10^{-3}$ v (as in Fig. 6). Applying equation 2:

$$40 \times 10^{-6} \text{ F/cm}^2 \times (-47 \text{ v/sec}) = -0.078 \text{ mho/cm}^2 (141.2 \times 10^{-3} \text{ v})$$
$$-0.129 \text{ mho/cm}^2 (49.2 \times 10^{-3} \text{ v} - E_{Na}).$$
$$E_{Na} = 122 \times 10^{-3} \text{ v}.$$

Conductances and Currents during Spike

At first impedance peak:

$$V = 67.2 \times 10^{-3} \text{ v}; \; dV/dt = 36.6 \text{ v/sec}.$$

Applying equation 2:

$$40 \times 10^{-6} \text{ F/cm}^2 \times 36.6 \text{ v/sec} = -0.078 \text{ mho/cm}^2 (159 \times 10^{-3} \text{ v})$$
$$-G_{Na} (-54.8 \times 10^{-3} \text{ v}).$$

1. $G_{Na} = 0.251$ mho/cm².
2. $G_L + G_{Na} = 0.329$ mho/cm² (Fig. 10).
3. $I_{Na} = G_{Na} (V - E_{Na}) = -13.8$ ma/cm² (Fig. 9).
4. $I_L = G_L (V + E_K) = 12.4$ Na/cm² (Fig. 9).
5. $I_{total} = I_{Na} + I_L = -1.4$ ma/cm² (Fig. 9).

At secondary impedance peak:

$$V = -18.5 \times 10^{-3} \text{ v}; \; G_L \cong G_{total}$$

6. $I_L = 0.078$ mho/cm² $(73.5 \times 10^{-3}$ v) $= 5.83$ ma/cm².

At time of peak outward current:

$$dV/dt = -194 \text{ v/sec}; \; V = -38.4 \times 10^{-3} \text{ v}$$
$$-40 \times 10^{-6} \text{ F/cm}^2 \times 194 \text{ v/sec} = (-0.078 - G_K) \text{ mho/cm}^2 \times 53.6 \times 10^{-3} \text{ v}.$$

7. $G_K = 0.067$ mho/cm² (Fig. 10).
8. $G_K + G_L = 0.145$ mho/cm² (Fig. 10).
9. $I_K = 3.57$ ma/cm² (Fig. 9).
10. $I_L = 4.18$ ma/cm² (Fig. 9).
11. $I_{total} = 7.75$ ma/cm² (Fig. 9).

Work in this Laboratory is supported in part by a grant from the Muscular Dystrophy Associations of America; by Public Health Service Research Grants NB 03728, NB 03270 and Training Grant NB 5328, from the National Institute of Neurological Diseases and Blindness; and by a grant from the National Science Foundation (G-2940).

Dr. Morlock was a USPH Fellow and is now in the Department of Neurophysiology, Walter Reed Army Institute of Research, Washington, D. C. 20012 (until October 1, 1968). We thank Dr. George M. Katz and Mr. Bernard Kline for their assistance and for helpful discussions.

Received for publication 30 October 1967.

REFERENCES

ADRIAN, R. H. 1964. The rubidium and potassium permeability of frog muscle membrane. *J. Physiol.* (*London*). **175**:134.

ALTAMIRANO, M., and C. W. COATES. 1957. Effect of potassium on electroplax of *Electrophorus electricus*. *J. Cellular Comp. Physiol.* **49**:69.

ALTAMIRANO, M., C. W. COATES, and H. GRUNDFEST. 1955. Mechanisms of direct and neural excitability in electroplaques of electric eel. *J. Gen. Physiol.* **38**:319.

BENNETT, M. V. L. 1961. Modes of operation of electric organs. *Ann. N. Y. Acad. Sci.* **94**:458.

BENNETT, M. V. L., and H. GRUNDFEST. 1959. Electrophysiology of *Sternopygus* electric organ. Proceedings 21st International Congress of Physiological Sciences, Buenos Aires. 35. (Abstr.)

BENNETT, M. V. L., and H. GRUNDFEST. 1961. Studies on morphology and electrophysiology of electric organs. III. Electrophysiology of electric organs in Mormyrids. *In* Bioelectrogenesis. C. Chagas and A. Paes de Corvalho, editors. Elsevier Publishing Co., Amsterdam. 113.

BENNETT, M. V. L., and H. GRUNDFEST. 1966. Analysis of depolarizing and hyperpolarizing inactivation responses in gymnotid electroplaques. *J. Gen. Physiol.* **50**:141.

COLE, K. S., and R. H. COLE. 1936. Electric impedance of *Asterias* egg. *J. Gen. Physiol.* **19**:609.

COLE, K. S., and H. J. CURTIS. 1939. Electric impedance of the squid giant axon during activity. *J. Gen. Physiol.* **22**:649.

EHRENSTEIN, G., and D. L. GILBERT. 1966. Slow changes of potassium permeability in the squid giant axon. *Biophys. J.* **6**:553.

GRUNDFEST, H. 1957. The mechanisms of discharge of the electric organs in relation to general and comparative electrophysiology. *Progr. Biophys.* **7**:1.

GRUNDFEST, H. 1961. Ionic mechanisms in electrogenesis. *Ann. N. Y. Acad. Sci.* **94**:405.

GRUNDFEST, H. 1963. Impulse conducting properties of cells. *In* The General Physiology of Cell Specialization. D. Mazia and A. Tyler, editors. McGraw-Hill Book Co., New York. 277.

GRUNDFEST, H. 1966 *a*. Comparative electrobiology of excitable membranes. *In* Advances in Comparative Physiology and Biochemistry. O. E. Lowenstein, editor. Academic Press Inc., New York. **2**:1.

GRUNDFEST, H. 1966 *b*. Heterogeneity of excitable membrane: Electrophysiological and pharmacological evidence and some consequences. *Ann. N. Y. Acad. Sci.* **137**:901.

GRUNDFEST, H. 1967. Some comparative biological aspects of membrane permeability control. *Federation Proc.* **26**:1613.

HODGKIN, A. L., and A. F. HUXLEY. 1952. A quantitative description of membrane current and its application to conduction and excitation in nerve. *J. Physiol.* (*London*). **117**:500.

JENERICK, H. 1963. Phase plane trajectories of the muscle spike potential. *Biophys. J.* **3**:363.

KATZ, B. 1966. Nerve, Muscle, and Synapse. McGraw-Hill Book Co., New York.

KEYNES, R. D., and H. MARTINS-FERREIRA. 1953. Membrane potentials in the electroplates of the electric eel. *J. Physiol.* (*London*). **119**:315.

MORLOCK, N., D. A. BENAMY, and H. GRUNDFEST. 1967. Phase plane and AC impedance analysis of the action potential in space-clamped isolated electroplaques of the electric eel. *J. Gen. Physiol.* **50**:2488. (Abstr.)

NAKAMURA, Y., and H. GRUNDFEST. 1965. Different effects of K and Rb on electrically excitable membrane of eel electroplaques. Proceedings 23rd International Congress of Physiological Sciences, Tokyo. 167. (Abstr.)

NAKAMURA, Y., S. NAKAJIMA, and H. GRUNDFEST. 1965. Analysis of spike electrogenesis and depolarizing K-inactivation in electroplaques of *Electrophorus electricus*, L. *J. Gen. Physiol.* **49**:321.

NAKAJIMA, S., and K. KUSANO. 1966. Behavior of delayed current under voltage-clamp in the supramedullary neurons of puffer. *J. Gen. Physiol.* **49**:613.

NISHI, S., H. SOEDA, and K. KOKETSU. 1965. Studies on sympathetic B and C neurons and patterns of preganglionic innervation. *J. Cellular Comp. Physiol.* **66**:19.

SHANES, A. M., H. GRUNDFEST, and W. FREYGANG. 1953. Low level impedance changes following the spike in the squid giant axon before and after treatment with "veratrine" alkaloids. *J. Gen. Physiol.* **37**:39.

TYLER, A., A. MONROY, C. Y. KAO, and H. GRUNDFEST. 1956. Membrane potentials and resistance of the starfish egg before and after fertilization. *Biol. Bull.* **111**:153.